Bethe Surface and Inelastic and Elastic Differential Cross Sections for Helium Obtained by Use of 25-keV Incident Electrons*†

H. F. Wellenstein, R. A. Bonham, and R. C. Ulsh
Department of Chemistry, Indiana University, Bloomington, Indiana 47401
(Received 11 September 1972)

The complete electron-impact spectra, including the elastic scattering, for He have been obtained at the scattering angles 1°, 1.5°, 2°, 3°, 4°, 5°, 7°, and 10° using 25-keV incident electrons. The data cover the momentum-transfer region from 0.8 to 7.5 in atomic units (a.u.). Measured intensities were converted approximately to relative generalized oscillator strengths for different values of energy transfer, and placed on an absolute scale by use of the Bethe sum rule. Although sum-rule normalization using the energy-loss spectrum at a fixed angle is not rigorous, it is justified in the large-angle high-energy limit. Comparison of the results with the theory proved that use of sum-rule normalization was justified at angles as small as 1°. The first-Born theory was shown to be in agreement with experiment over the complete data range. In the case of the binary-encounter theory, good agreement with experiment was obtained from momentum-transfer values greater than 4 a.u. Below 4 a.u. substantial deviations were observed, especially in regions removed from the maximum of the spectral distribution. Sums of the generalized optical-oscillator strength, the x-ray incoherent-scattering factor $S(K)$, the elastic differential, and total scattering cross sections were all computed from the experimental data. The experimental values of $S(K)$ and the elastic differential cross section agreed with accurate theoretical calculations to an average accuracy of 2%. Compton profiles obtained at 5°, 7°, and 10° were found to be in excellent agreement with previous electron-impact, x-ray, and γ-ray measurements. The unresolved autoionizing double excitations ($2s2p$, $2p^2$, etc.) at an energy loss of 60 eV were observed at both 1° and 2.7°. The $2^1P \leftarrow 1^1S$ transition at 21.2 eV was also a prominent feature of the Bethe surface and could still be observed at angles as large as 4°.

I. INTRODUCTION

The generalized oscillator strength $f_n(K)$, which is related to the angular dependence of the differential cross section for structureless charged-particle collisions with atoms or molecules within the framework of the first-Born approximation of scattering theory, may be defined as[1]

$$f_n(K) = E_n \left| \left\langle \Psi_n \right| \sum_{i=1}^{N} e^{i\vec{K}\cdot\vec{r}_i} \left| \Psi_0 \right\rangle \right|^2 K^2 \qquad (1)$$

for bound-state transitions. For a transition into a continuum state it is more convenient to use the density of the generalized oscillator strength per unit range of energy loss E, which is defined as[1]

$$\frac{df(E,K)}{dE} = \sum_n E_n \left| \left\langle \Psi_n \right| \sum_{i=1}^{N} e^{i\vec{K}\cdot\vec{r}_i} \left| \Psi_0 \right\rangle \right|^2 \delta(E_n - E) \Big/ K^2 \ , \qquad (2)$$

where E_n is the energy gained by the target on being excited from its ground state to its nth excited state, or the energy loss suffered by the incident electron, K is the momentum transfer to the target by a charged particle, $\vec{r}_i$ defines the instantaneous position of the ith of N target electrons, and Ψ_n and Ψ_0 are wave functions describing the target in its final and initial states, respectively. In Eqs. (1) and (2) as well as in later equations, energies are measured in Ry and momentum transfer in units of $\hbar$, unless otherwise stated. In the case of high-energy electron scattering, both exchange and relativistic effects must be considered in relating Eqs. (1) and (2) to the differential cross section.[2]

A plot of the generalized oscillator strength as a function of energy loss and the logarithm to the base e of the square of the momentum transfer defines a surface, called the Bethe surface,[3] which contains the information necessary to predict within the framework of the first-Born scattering theory the behavior of matter under charged-particle impact.[1] Such quantities as the high-energy asymptotic form of the total inelastic scattering cross section for incident charged particles in the first-Born approximation,[1] the stopping power,[1] the total inelastic differential cross section,[2] the Compton profile,[4,5] and the Fourier transform of certain target charge densities[6] can be obtained from an accurate knowledge of the Bethe surface. In spite of the obvious utility of the Bethe surface, only the theoretical Bethe surface for the hydrogen atom has been reported to date.[1]

The work presented here represents the first reasonably complete experimental determination

of a Bethe surface under conditions in which the first-Born theory of scattering should be valid. High-energy electron-impact spectroscopy has been chosen as the most appropriate means of obtaining such information in spite of the complicating aspects of relativistic and exchange corrections. It is felt that the ready availability of high-intensity, reasonably monoenergetic electron sources and suitable detectors at incident electron energies in the keV range more than make up for any disadvantages.

Previous work carried out in this laboratory and elsewhere give adequate testimony to the successful use of keV incident-energy electrons to obtain small-angle ($<2°$) intensities which correlate well with the predictions of the first-Born theory.[7,8] In addition, Refs. 4 and 5 describe larger-angle measurements (7°, 25°, 35°, and 45°), some of which were carried out at different incident energies. Unfortunately these results do not provide a fine enough mesh in scattering angle or momentum transfer to adequately document a Bethe surface.

II. THEORY

The connection between the generalized oscillator strength and the Bethe surface has been adequately treated elsewhere.[1] The connection between the generalized oscillator strength and the cross-section differential with respect to the solid angel of the scattered electron and energy loss of the incident electron, referred to here as the double differential cross section $d^2\sigma(E,K)/dEd\Omega$, can be written approximately as[2]

$$\frac{df(E,K)}{dE} = \frac{Ek(K^2 - E^2/4c^2)^2(1-\beta^2)}{4[1-E(1-\beta^2)^{1/2}/2c^2]k(E)K^2F_{ex}^R}\frac{d^2\sigma(E,K)}{dEd\Omega}, \tag{3}$$

where E is the energy loss, c is the velocity of light, β is the ratio of the incident electron velocity to the velocity of light, k and $k(E)$ are the incident and scattered momenta, respectively, K is the momentum transfer from the incident electron to the target on scattering which is a function of E, and F_{ex}^R is a correction for exchange. The exchange correction can be written approximately as[2]

$$F_{ex}^R = 1 - \frac{K^2 - E^2/4c^2}{[k^4 + 4k^2(E)(q^2 - qq' - \Delta/8c^2) + qq'\Delta/c^2 + \Delta^2/16c^4]^{1/2}} + \frac{(K^2 - E^2/4c^2)^2[k^2(E) - 2qq' - \Delta/4c^2]}{[k^4 + 4k^2(E)(q^2 - qq' - \Delta/8c^2) + qq'\Delta/c^2 + \Delta^2/16c^4]^{3/2}}, \tag{4}$$

where

$$q = \frac{E - (K^2 - E^2/4c^2)}{2K}, \quad q' = \frac{k(E)k\cos\theta - k^2(E)}{K},$$

and $\Delta = (E_0 - E)^2$, in which E_0 is the energy of the incident electron and $E_0 - E$ is the energy of the scattered electron.

As pointed out in Ref. 2, the experimental cross section $(d^2\sigma/dEd\Omega)_{expt}$ can be placed on an absolute scale, provided that the first-Born approximation is valid and that the energy-loss width of the inelastic spectrum is sufficiently narrow so that

$$\frac{df(E,K)}{dE} \approx \frac{df}{dE}(E,\bar{K}),$$

where $\bar{K}$ is evaluated at the energy loss $\bar{E}$ which can be conveniently taken as the value for which the inelastic cross section is a maximum for the particular angle under consideration. These assumptions will be tested experimentally in this paper. If these conditions are satisfied, then Eq. (3) can be used to obtain the generalized oscillator strength; and the Bethe sume rule[1]

$$\int dE \frac{df(E,\bar{K})}{dE} = N, \tag{5}$$

where N is the number of electrons in the target system, can be used to put the experimental data on an absolute scale. The double differential cross section and generalized oscillator strength may then be plotted and compared with theory. As a by-product of the inelastic scattering measurements, the elastic scattering as a function of scattering angle is also usually observed. It is then possible to integrate both elastic and inelastic scattering over energy loss to obtain the corresponding cross-sections differential with respect to the solid angle of the scattered electron. In addition, the inelastic cross-section differential with respect to energy loss can be obtained by integrating the double differential cross section over scattering angle.

In the process of normalizing the data by use of the Bethe sum rule, it is of interest to obtain some of the other closely related sums[1]:

$$S(\mu,K) = \int dE \frac{E^\mu df(E,K)}{dE}. \tag{6}$$

The sum $S(-1,K)$ is related to the familiar x-ray incoherent-scattering factor $S(K)$ by[1]

$$S(-1,K) = S(K)/K^2, \tag{7}$$

which approaches the limit N/K^2, where N is the total number of target electrons, as $K \to \infty$. In addition, the limits[1] $\lim_{K\to\infty} S(1, K) = NK^2$ and $\lim_{K\to\infty} S(2, K) = NK^4$ are known and should prove useful in checking experimental data for consistency. Another useful check in this regard is the sum-rule inequality[1]

$$S(\mu, K)^2 \leq S(\mu - \nu, K)S(\mu + \nu, K) . \quad (8)$$

Note that since the equality holds in the limit as $K \to \infty$, it is possible to show by recurrence[1] that $\lim_{K\to\infty} S(\mu, K) = NK^{2\mu}$.

Perhaps the most prominent feature of the Bethe surface is the Bethe ridge,[1] whose maximum position is given by conservation of energy and momentum for a binary collision. The ridge position is given by $E = K^2$ by nonrelativistic kinematics and by $E = Q = K^2 - E^2/4c^2$ by relativistic kinematics.[1,2] A cut through the Bethe ridge at a constant scattering angle is given approximately by the binary-encounter theory as[2]

$$\frac{d^2\sigma}{dEd\Omega} = \frac{2k(E)[1 - E(1-\beta^2)^{1/2}/2c^2]F_{ex}^R J'(q)}{k(1-\beta^2)K(K^2 - E^2/4c^2)^2} , \quad (9)$$

where

$$J'(q) = 2\pi \int_q^\infty dp\, p\{\rho(p) - \tfrac{1}{2}F(K)\rho([p^2 + k^2 - k^2(E)]^{1/2}, p)\} \quad (10)$$

for a Hartree–Fock description of the He-atom ground state, where $\rho(p)$ is the diagonal one-electron momentum density, $\rho(p', p)$ is the nondiagonal one-electron momentum density, and $F(K)$ is the x-ray coherent-scattering factor. The first term in Eq. (10), usually written as

$$J(q) = 2\pi \int_q^\infty dp\, p\rho(p) , \quad (11)$$

is the x-ray Compton profile which can be extracted from a cross section taken at constant scattering angle of the large-angle Bethe ridge—providing that relativistic and exchange corrections are adequate[4,5] and the binary-encounter theory is valid. Since the binary-encounter theory is a more severe approximation than the first-Born scattering theory,[1,2] it is of some interest in the present experimental work to try to ascertain its limits of validity.

The study of Compton profiles is of interest by itself,[4,5] and it only needs to be pointed out here that every cross section of the Bethe ridge at constant angle, once the region of validity of the binary-encounter theory is reached, contains all the information necessary to determine the total electronic energy of the target system in addition to several moments of the target-electron momentum density as well as the momentum density itself.[2,9]

III. EXPERIMENTAL

The experimental apparatus[10] has been described in part elsewhere.[4] An electron gun of the telefocus type[11,12] was mounted inside a large vacuum chamber on an arm rotatable through 180° about a gas jet formed by expansion of the gas through a hypodermic needle with an inside diameter of 0.125 mm. The center of the scanning arm was directly coupled to a ±0.01% linear potentiometer, used for measuring the scattering angle, and the arm was carefully aligned with respect to rotation about the center of the gas jet. Careful calibration of the angle measurement indicated that the scattering angle was accurate to about ±0.01°.[13] A specially designed highly efficient electron trap was employed to collect unscattered electrons.

Two sets of collimating slits, a velocity analyzer, and a detector were mounted in their own smaller vacuum chamber which was fastened at a horizontal viewing port to the large-vacuum system. The velocity analyzer was of the Möllenstedt type[14,15] and a silicon solid-state detector[4] was used for counting the scattered electrons. A variable bias voltage was floated on top of the incident-electron-beam accelerating voltage and the sum was applied to the center electrode of the Möllenstedt analyzer. By varying the bias voltage the energy-loss spectrum could be electronically scanned across the detector entrance slit. The spectra were signal averaged with one sweep of the spectrum, usually carried out in less than 1 min. The best resolution of the analyzer was about 300 meV, but the energy spread of the unmonochromatized incident electron beam limited the actual resolution to about 600 meV. It proved a simple matter to degrade the resolution to improve counting statistics when necessary. The high-voltage power supply used to produce the incident electron beam was regulated to ±0.01%/h and the acceleration potential was determined[16] within 0.01%. The fact that the accelerating voltage was also connected to the center of the Möllenstedt analyzer caused fluctuations in the accelerating voltages to cancel out. The elastic peak was scanned across the spectrum with known bias voltages in order to provide calibration markers for the energy-loss scale.

The target gas-flow rates into the scattering chamber were measured and adjusted to yield maximum counting rates consistent with manageable dead time and multiple scattering corrections. Pressures without the presence of target gas were on the order of 3×10^{-7} Torr. The scattering chamber pressure varied between 2×10^{-4} and 3×10^{-5} Torr during data collection with He, depending on the particular flow rate used. The velocity-analyz-

er chamber pressure always remained below 2 $\times 10^{-6}$ Torr during the experiments.

Experimental conditions used in data collection consisted of electron beam currents of 100 μA at scattering angles of 4°, 5°, 7°, and 10° and 20 μA at 1°, 1.5°, 2°, 3°, and 4° with gas-flow rates of 1×10^{20} atoms/sec at 7° and 10°, and 1.5×10^{19} atoms/sec at 1°, 1.5°, 2°, 3°, 4°, 5°, and 7°. Identical conditions were employed for the angles 1°, 4°, 7°, and 10° measured on the opposite side of the zero angle. Reported measurements at the same angle under different electron-beam and gas-flow conditions made it possible to obtain realistic estimates of the reproducibility of the experimental data.

The problem of detector entrance slit geometry and the finite size of the scattering volume have been treated elsewhere.[17] For the geometries considered in this experiment the calculated correction for finite scattering volume and detector slit geometry was found to be less than 0.3%. A further correction was necessary owing to the field-sweeping mode of the analyzer; the intensity of the spectrum was multiplied by $E_0/(E_0-E)$, a correction of 4% at the highest energy loss encountered.[18]

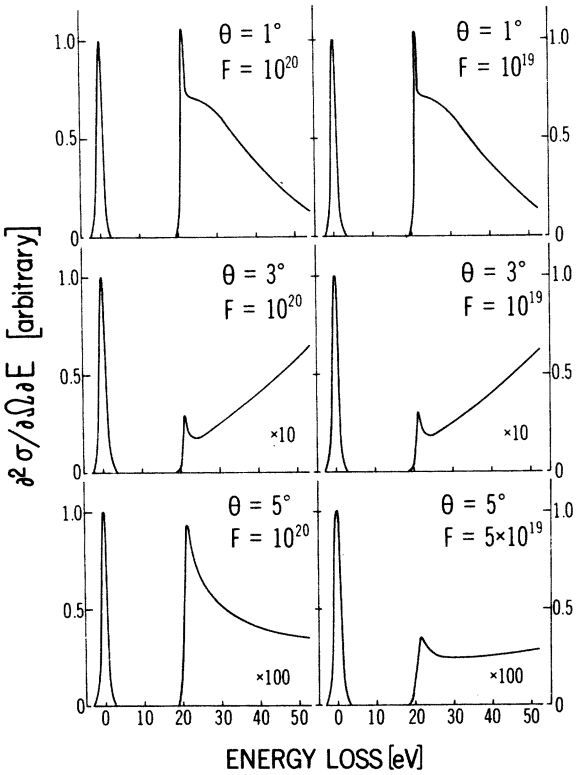

FIG. 1. Effect of multiple scattering for scattering angles of 1°, 3°, and 5°. Two flow rates F (atoms/sec) were used at each angle. The scales for the ordinates of the plots were determined by setting the maximum of the elastic line (energy loss equals zero) to unity. Multiple scattering does not contribute at 1° and 3°, but contributes significantly at 5° in the spectral range shown. The contribution to the total inelastic profile is only 0.5% at 5°. The ×10 and ×100 signifies that the inelastic part of the spectrum has been magnified 10 or 100 times compared to its actual value.

Corrections to the data for the dead time of the detection system were routinely made. The dead time τ of the system was found to be 3.05 ± 0.02 μsec, which was reproducible over a time span of at least several weeks of constant use within the stated uncertainty. In actual experiments the maximum count rate was never allowed to exceed 125 kHz.

Another potentially serious source of experimental uncertainty is multiple interatomic scattering. The presence or absence of multiple scattering was determined by recording the energy-loss spectrum for He, including the elastic line, from 0 to 50 eV at two different gas-flow rates. The results of these tests are shown in Fig. 1. Only the 5° spectrum shows any effect from multiple scattering and even in this case the contribution to the significant part of the inelastic spectrum amounts to less than 0.5%.

The Bethe sum rule, Eq. (5), is strictly valid only when the sum over energy loss is carried out at constant momentum transfer. Since the present measurements were obtained at constant angle, an experimental test was carried out to determine whether the sum rule could be approximately employed with our data. Calculations indicated that the sum rule should be valid at larger scattering angles[1] (> 5°, where K is independent of the energy loss E over the spectral range at the 0.1% accuracy level). It was decided that the sum rule could be tested at the smaller scattering angles in two ways.

First, the most direct method was to use the sum-rule normalization at 10° and use careful measurements of all experimental parameters to place the other angle measurements on the same intensity scale. These results could then be compared with the separate use of the Bethe sum rule at each different scattering angle. Second, a further check was made by comparing the results for the sum rule given in Eq. (7) and the elastic cross section with accurate theoretical values for both sets of normalized data.

In order to put data for different scattering angles on the same scale, it was essential to make careful assessments as to background scattering contributions (scattering from regions outside the gas jet) in addition to dead-time corrections, interatomic multiple scattering corrections, and corrections to the scattering-angle measurement.

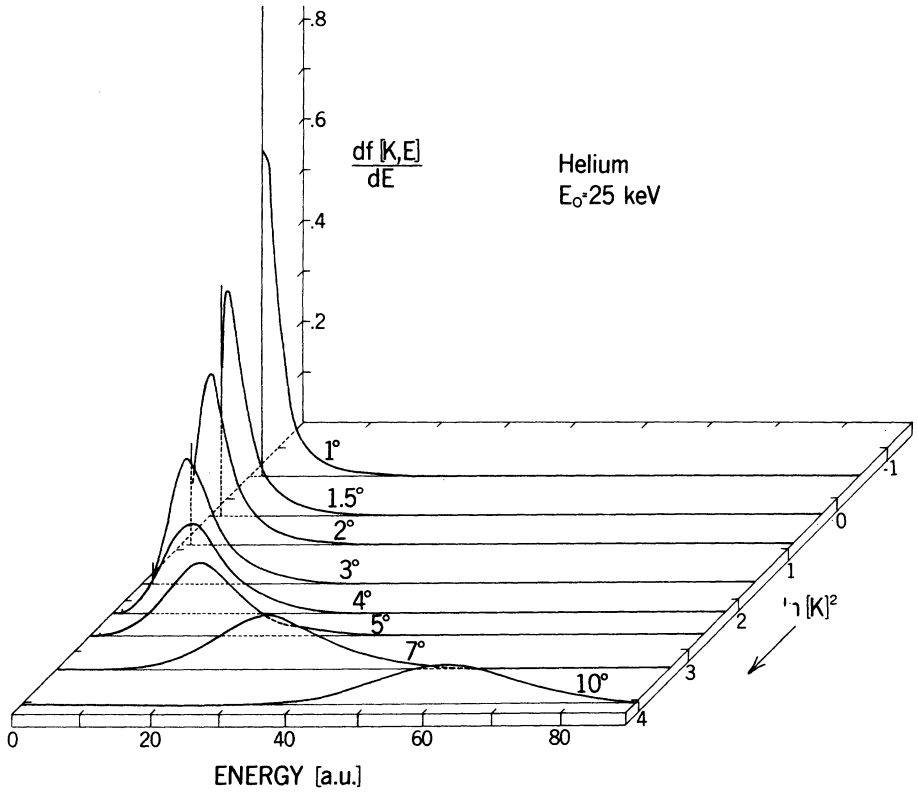

FIG. 2. Bethe surface of helium obtained with 25-keV electrons. Experimental cross sections were converted to generalized oscillator strengths (a.u.) by use of Eq. (3), and the data were placed on an absolute scale using the Bethe sum rule.

Experiments showed that the background scattering consisted of two parts. The first was an essentially constant background contribution as a function of energy loss varying from less than 0.1% of the maximum scattered intensity at 1° scattering angle to 1% at 10°. This contribution is readily observable by scanning over a spectral range in excess of the energy range of the actual spectrum. Possible sources for this background are detector noise, multiple scattering from chamber walls, low-energy cosmic radiation, and scattering off aperture edges. Obviously it is a simple matter to correct experimental data for this source of background scattering.

The second source comes from scattering in regions near the volume of intersection of the gas jet

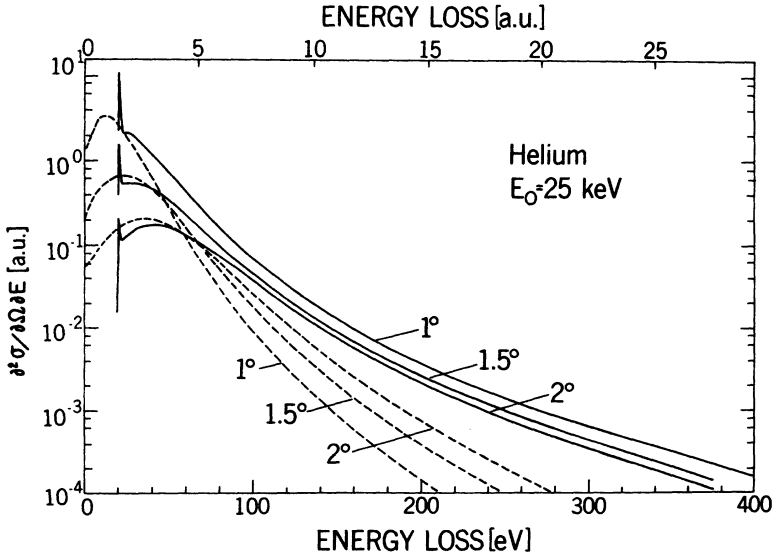

FIG. 3. Cross-section (a.u.) differential with respect to energy loss (a.u.) and scattered solid angle plotted as a function of energy loss (a.u.) at angles of 1°, 1.5°, and 2°. The solid line refers to experiment and the dotted line to binary-encounter theoretical values.

and electron beam. In order to collect data over the angular range 1° –10° with comparable accuracy and to keep all the data on the same relative scale, it is essential to frequently change the electron- and gas-beam densities. Since such changes cannot be made without introducing slight changes in the scattering volume, it is necessary to look at a volume in excess of the maximum volume encountered in the experiment. Experiments showed that scattering from regions adjacent to the gas jet contributed a background with a shape nearly identical to that of the actual energy-loss spectrum. As expected the magnitude of the correction varies strongly with scattering angle ranging from 10% at 1° to 2% at 10°.

The results of the two normalization procedures were in agreement with a maximum error of 4% and an average error of 2% for the angles studied (1°, 1.5°, 2°, 3°, 4°, 5°, 7°, and 10°). In addition, the experimental x-ray incoherent-scattering factors derived from these data, as discussed in detail in Sec. IV (see Table IV), were found to be in excellent agreement with theory (2% average agreement). Two observations are worth mentioning here. When the two methods of normalization were compared without proper correction for background scattering, up to 15% deviations were observed for the resultant x-ray incoherent-scattering values. Use of the Bethe sum rule at each separate scattering angle, on the other hand, yielded essentially the same result whether or not the background correction of the second kind was made. This was, of course, a consequence of the fact that this correction had nearly the same shape as the observed spectrum.

We feel that these results justify use of the Bethe sum rule over the angular range studied at an incident electron energy of 25 keV to an accuracy of at least 2%. This means that by closing down the slit closest to the scattering volume, the background correction of the second kind can be eliminated in future experiments. The data for each angle can then be separately scaled by use of the Bethe sum rule. It is not clear whether this conclusion will also hold for heavier systems, since the spectral width will increase and the variation in momentum transfer with energy loss over the spectral range will be larger. An independent argument, supporting the conclusions reached here is given in connection with Eq. (12) in the next section.

IV. RESULTS

The experimental cross sections were converted to generalized oscillator strengths, Eq. (3), and the data were placed on an absolute scale by use of the Bethe sum rule (see Sec. III for the experimental details). In Fig. 2 the final results of this work are summarized by a plot of the data in the form of a Bethe surface. The Bethe ridge and the angular dependence of the $2^1P \leftarrow 1^1S$ transition are the most prominent features of this surface. A less prominent feature of the surface was the observation of a resonance-type transition at 60 eV. This transition will be discussed in more detail at the end of this section. These features illustrate one important reason for attempting to obtain measurements of a complete Bethe surface. That is, a Bethe surface can be regarded as a survey which will turn up all reasonably prominent energy-loss mechanisms and hence provide significant direction for future experimental work.

In Figs. 3 and 4 the cross-sections differential with respect to scattered energy loss and solid angle are plotted as a function of energy loss. Those values were placed on an absolute scale by use of the Bethe sum rule and are compared to theoretical calculations based on a first-Born binary-encounter theory (dotted lines) utilizing an approxi-

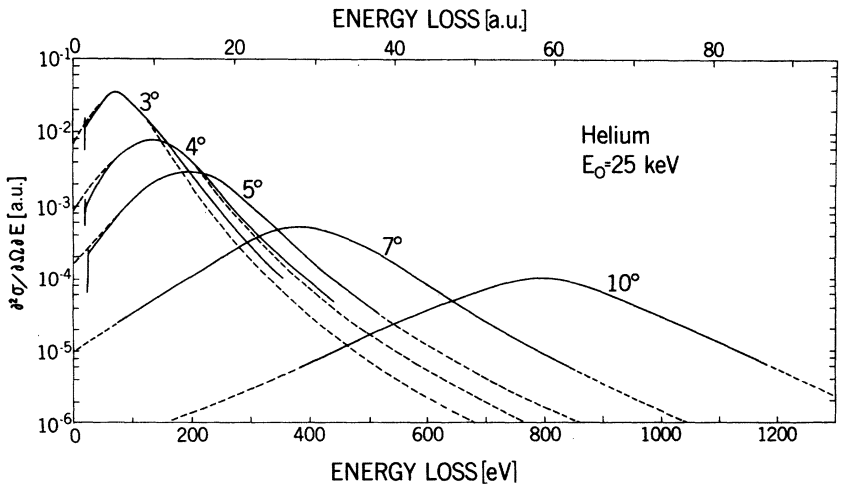

FIG. 4. Cross-section (a.u.) differential with respect to energy loss (a.u.) and scattered solid angle plotted as a function of energy loss (a.u.) at angles of 3°, 4°, 5°, 7°, and 10°. The solid line refers to experiment and the dotted line to binary-encounter theoretical values.

mate Hartree–Fock wave function. The agreement between theory and experiment is excellent at the scattering angles of 5°, 7°, and 10° with increasing deviations for smaller angles.

In Fig. 5 the same data are plotted as a function of both K and $\ln[K^2]$ for fixed energy loss. It is clear from this plot that the binary-encounter theory breaks down for momentum-transfer values less than 4 a.u. In Table I our experimental values at 1°, 1.5°, and 2° for energy losses of 28.5, 41.8, and 54.3 eV are compared with the complete first-Born theoretical values of Oldham.[19] The results agree with experiment within 10% for all cases studied. At 1°, experimental values from the work of Silverman and Lassettre[20] have also been compared with our results.

Our results show that the first-Born theory and experiment are in excellent agreement and that the binary-encounter model fails at small scattering angles. Note also that in spite of the large deviations at small angles, the binary-encounter model is still in relatively good agreement with theory at the maximum of the Bethe surface. It is also of interest to note that the total inelastic differential cross section derived from the binary-encounter theory [Eqs. (9) and (10)] agrees with the experimental and first-Born values to within 10% in spite of the serious disagreement for the case of the double differential cross section. In terms of the binary-encounter model, those scattered electrons contributing to the maximum of the inelastic distribution—which may also be referred to as the Compton peak—have collided mainly with target electrons possessing zero momentum. It is precisely for such collisions that the binary-encounter model should be valid. Vriens[21] showed theoretically that the binary-encounter and first-Born theories agreed for $K > 3$ a.u. for the H atom. This study provides the first experimental comparison of this kind for the He atom.

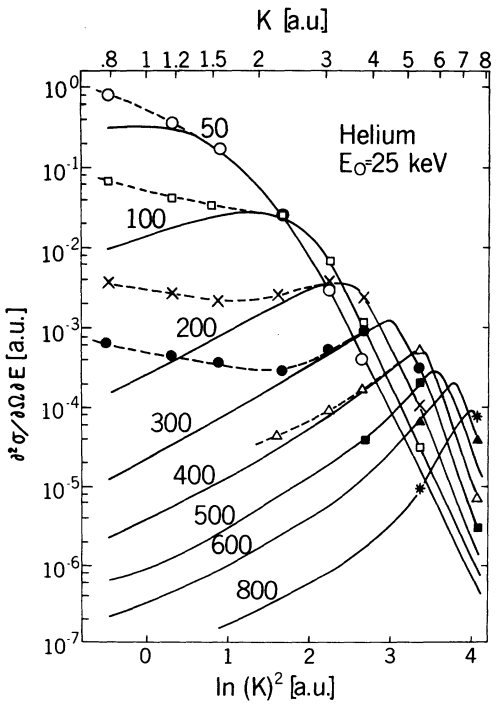

FIG. 5. Cross-section (a.u.) differential with respect to energy loss (a.u.) and scattered solid angle plotted as a function of momentum transfer (a.u.) for energy losses of 50, 100, 200, 300, 400, 500, 600, and 800 eV. The solid lines are obtained by binary-encounter theory, Ref. 2. This plot indicates the breakdown of binary-encounter theory for momentum-transfer values less than 4 a.u.

It has been pointed out that there may be deviations between the experiment and the first-Born theory at large scattering angles coming from higher Born corrections involving coupling with the elastic channel.[22] Such deviations were not observed here except possibly for the $2^1P - 1^1S$ transition, but this work cannot be considered a definitive test of the presence or absence of such effects except that they appear to be absent at the 10–15% level (percent of maximum inelastic intensity at same scattering angle) for $4° \leq \theta \leq 10°$ in the observed range.

The cross sections of the Bethe ridge at 5°, 7°, and 10° were all analyzed in terms of the Compton profile $J(q)$. The high-energy-loss side, including the peak maximum, were found to be in excellent agreement with previous studies in each of the three cases.[5] Integration of $J(q)$ over the range $0 \leq q \leq \infty$ (assuming a dependence of q of the form q^{-6} for values of q greater than 4) yielded a value very close to unity in each case.

As a by-product of normalizing the experimental data by use of the Bethe sum rule $S(0, K)$, the additional sums $S(2, K)$, $S(1, K)$, $S(-1, K)$, and $S(-2, K)$

TABLE I. Generalized oscillator strength $df(K, E)/dE$ as a function of momentum transfer K, comparing the present experimental values (a) with the first-Born theoretical results of Oldman (Ref. 19) (b) and the experimental results of Silverman and Lassettre (Ref. 20) (in parentheses). The momentum-transfer values used for the results of Oldham and of Silverman and Lassettre are those given by the authors, and for (a) the K values were computed according to the formula $K^2(E) = 2k^2 - E - 2k(k^2 - E)^{1/2} \times \cos\theta$.

	$E = 28.5$ eV		$E = 41.8$ eV		$E = 54.3$ eV	
K	(a)	(b)	(a)	(b)	(a)	(b)
0.79	0.632 (0.561)	0.581	0.485 (0.45)	0.440	0.311 (0.37)	0.293
1.17	0.370	0.357	0.437	0.427	0.362	0.353
1.55	0.180	0.170	0.304	0.304	0.351	0.342

TABLE II. Experimental sum-rule values for helium using the $S(0,K)$ sum for placing the experimental data on an absolute scale. Values of K were computed as described in the caption to Table I.

Scattering angle (deg)	K (a.u.)	$S(2,K)$	NK^{4} [a]	$S(1,K)$	NK^{2} [b]	$S(-1,K)$	NK^{-2} [c]	$S(-2,K)$	NK^{-4} [d]
	0	121.336[e]		8.16745[e]		0.752498[e]		0.3459[f]	
1	0.795	62 ± 2[g]	0.799	8.9 ± 0.2	1.26	0.61 ± 0.02	3.16	0.24 ± 0.1	5.01
1.5	1.174	75 ± 3	3.80	10.1 ± 0.4	2.76	0.54 ± 0.02	1.45	0.19 ± 0.1	1.05
2	1.552	105 ± 4	11.6	12.3 ± 0.5	4.82	0.44 ± 0.02	0.830	0.125 ± 0.10	0.345
3	2.309	181 ± 6	56.8	17.1 ± 0.6	10.7	0.30 ± 0.01	0.375	0.057 ± 0.003	0.0704
4	3.064	405 ± 15	176	26.1 ± 0.8	18.8	0.18 ± 0.01	0.213	0.024 ± 0.002	0.0227
5	3.819	700 ± 28	425	35.0 ± 1.0	29.2	0.133 ± 0.005	0.137	0.0112 ± 0.0005	9.40×10^{-3}
7	5.325	2130 ± 90	1608	63 ± 2	56.7	$(6.9\pm0.1)\times10^{-2}$	0.0705	$(2.7\pm0.1)\times10^{-3}$	2.49×10^{-3}
10	7.572	7850 ± 300	6574	123 ± 4	114.7	$(3.36\pm0.05)\times10^{-2}$	0.0349	$(5.9\pm0.2)\times10^{-4}$	6.08×10^{-4}

[a] $\lim K\to\infty$, $S(2,K)\to NK^{4}$.
[b] $\lim K\to\infty$, $S(1,K)\to NK^{2}$.
[c] $\lim K\to\infty$, $S(-1,K)\to NK^{-2}$.
[d] $\lim K\to\infty$, $S(-2,K)\to NK^{-4}$.
[e] C. L. Pekeris, Phys. Rev. 115, 1216 (1959).
[f] C. Schwartz, Phys. Rev. 127, 1700 (1961).
[g] The uncertainties are based on the precision of the experimental data and do not take into acout the error in assuming that K is independent of E. The error in $S(2,K)$ is on the order of 100 and 10% for $S(1,K)$ at $\theta=1°$, with smaller uncertainties as the angle increases. Uncertainties in $S(-1,K)$ and $S(-2,K)$ from this source are less than 0.1%.

were computed.[1] Values are shown in Table II along with the limiting forms for large momentum transfer. The uncertainties given in Table II are based only on the precision of the experimental data. Another source of error is the computation of the sums using data for a fixed angle rather than for fixed momentum transfer. It has been shown[23] that the μth sum over energy loss for fixed scattering angle can be written approximately in terms of sums for fixed momentum transfer as

$$S(\mu,\theta)=S(\mu,K)+\frac{\bar{E}^2}{4k_n^2}\frac{d}{dK^2}S(\mu,K)-\frac{\bar{E}}{2k_n^2}\frac{d}{dK^2}S(\mu+1,K)+\frac{1}{4k_n^2}\frac{d}{dK^2}S(\mu+2,K)+O\left(\frac{1}{k_n^4}\right), \qquad (12)$$

where K, k_n, and the derivatives of S are all evaluated at $\bar{E}$, the position of Bethe ridge maximum. The three correction terms to $S(\mu,K)$ given explicitly in Eq. (12) can be shown to vanish in the limit of large K. The results in Table II suggest that the errors arising from the assumption that generalized oscillator-strength sums computed at constant θ are the same as the sums computed at constant K in $S(0,K)$, $S(-1,K)$, and $S(-2,K)$ at $\theta=1°$ are 0.3, 0.04, and 0.005%, respectively. Note that these errors must be considered in addition to the experimental error estimates given in Table II. By extrapolation, $S(1,K)$ must be regarded as having errors from this source on the order of 5–10% and $S(2,K)$ with errors on the order of 50–100%. Of course, this source of error will decrease with increasing scattering angle.

In Table III the data are tested by use of the sum-rule inequality given in Eq. (8). All the results were found to be consistent to within the experimental uncertainties.

The sum rule $S(-1,K)$ is also simply related to the x-ray incoherent-scattering factor $S(K)$ [Eq. (7)] for which experimental values are compared with theory in Table IV. The theoretical wave function used in the calculation of $S(K)$ is an extremely

TABLE III. Experimental sum-rule inequalities for helium. Values of K were computed as described in the caption to Table I.

Scattering angle (deg)	K (a.u.)	$S^2(0,K)$ $\le S(-1,K)S(1,K)$	$S^2(0,K)$ $\le S(-2,K)S(2,K)$	$S^2(1,K)$ $\le S(0,4)S(2,K)$	$S^2(-1,K)$ $\le S(-2,K)S(0,K)$
1	0.795	4<5.5	4<14.9	79<116	0.37<0.48
1.5	1.174	4<5.4	4<14.3	102<150	0.29<0.38
2	1.552	4<5.4	4<13.1	151<210	0.19<0.25
3	2.309	4<5.1	4<10.3	292<362	0.090<0.114
4	3.064	4<4.7	4<9.7	681<810	0.032<0.048
5	3.819	4<4.6	4<7.8	1230<1400	0.018<0.0224
7	5.325	4<4.3	4<5.8	4000<4260	0.0048<0.0054
10	7.572	4<4.1	4<4.6	15000<15700	0.0011<0.0018

good one,[24] and the results can be considered as a calibration function for our experimental values. The average deviation of the fit of theory to experiment is less than ± 0.2% with apparent random sign changes, while the standard deviation for the fit is 2.1%. This would seem to suggest that there are no serious systematic sources of error present in our procedures and that the Born theory is valid at least to the 2% accuracy level.

The total experimental inelastic differential cross section is also plotted in Fig. 6 along with the theoretical values.[24] The disagreement between theory and experiment can no longer be observed on this insensitive plot. The reason for this plot is that one of the by-products of measuring the Bethe surface was the measurement of the elastically scattered intensity, and Fig. 6 provides an interesting comparison of the elastic and inelastic scattering. The elastic cross section was measured under identical conditions to those used for the inelastic scattering, but with a larger number of channels per eV used in the multichannel analyzer. The solid line in the elastic case represents theoretical results based on the first-Born approximation and a Hartree-Fock wave function. Note that the inelastic scattering dominates at small scattering angles, but that at large scattering angles the elastic scattering is approximately twice the inelastic, as would be expected on the basis of first-Born theory.

A resonance-like structure at 60 eV on the Bethe surface was also observed. Transitions in this energy-loss region have been extensively studied at low incident energies,[25] and Boersch *et al.*[26] have observed the $2s2p$ and $2s3p$ transitions at 50-meV energy resolution with 25-keV incident electrons at essentially zero scattering angle. We have now observed a structure in this same region using an experimental energy resolution of 2.0 eV out to angles as large as 2.7° ($K \sim 4$ a.u.). The results of two of our observations are shown in Fig. 7. The vertical lines labeled a, b, c, and d at the bottom of Fig. 7 label all the possible transitions in this region, while only the d-type transitions correspond to the optically allowed Rydberg-like series observed by Boersch and co-workers.[26] Because of the large angles and poor energy resolution used in this study, contributions from some of the optically forbidden transitions a, b, and c cannot be completely ruled out. The observation of the resonance-like structure at 2.7° can be quite accurately made,

TABLE IV. Experimental and theoretical values of the x-ray incoherent-scattering factor $S(K)$. Values of K were computed as described in the caption to Table I.

	$S(K)$		
K (a.u.)	Expt.[a]	Theory[b]	Deviation (%)
0.7197	0.347	0.346	+0.29
0.7951	0.392	0.410	−4.4
1.174	0.752	0.756	−0.53
1.552	1.060	1.046	+1.3
2.309	1.575	1.515	+0.40
2.990	1.736	1.745	−0.52
3.064	1.754	1.762	−0.45
3.823	1.951	1.884	+3.6
5.259	1.974	1.970	+0.20
5.334	1.992	1.972	+1.0
7.599	1.940	1.992	−2.6

[a] Experimental values for values of K not listed in Tables II and III were obtained by interpolation.
[b] Reference 24.

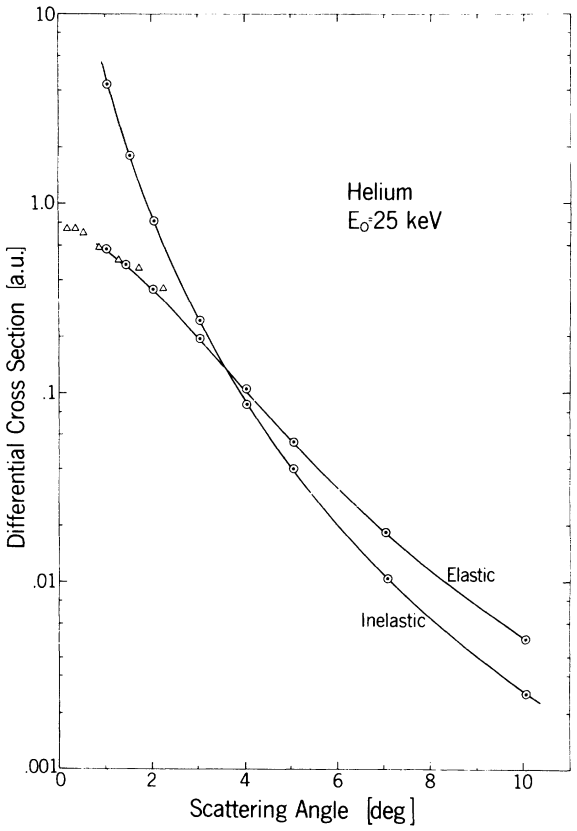

FIG. 6. Elastic and inelastic cross-sections differential with respect to scattered solid angle compared to theoretical values. The theoretical inelastic cross sections were calculated from the incoherent-scattering factors given by Kim and Inokuti (Ref. 24) using a very accurate ground-state wave function, while the elastic cross sections were calculated by the first-Born approximation using a Hartree-Fock (HF) wave function, since for the elastic case the differences between HF and more rigorous results are much smaller than experimental uncertainities. Relative measurements by Geiger (Ref. 29) (triangles) are shown, normalized to the same scale at 1.5°.

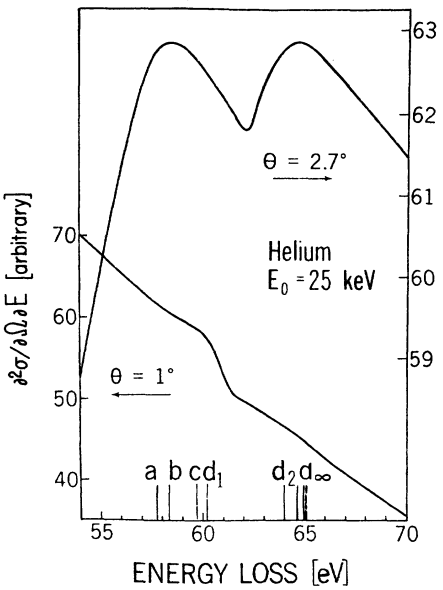

FIG. 7. Cross-section differential with respect to energy loss and scattered solid angle plotted in arbitrary units at scattering angles of 1° and 2.7°. The structure at about 60 eV is due to two-electron excitations; the vertical lines label all the possible transitions in this region. See text for further discussion.

because at this particular angle the maximum of the Bethe surface occurs at almost exactly 60 eV; hence good counting statistics can readily be obtained. As can be observed from Fig. 7 the ratio of the amplitude of the resonance to the background intensity corrected for the resolving power of the spectrometer with an assumed natural linewidth of 40 meV[27] at 1° ($K = 0.8$ a.u.) is about 5, and is 2 at 2.7° ($K = 2$ a.u.), which means that the ratio of the amplitude of the resonance to the background is falling off slightly faster than K^{-1} with increasing momentum transfer. This same parameter has been estimated to be 9 from photoabsorption data[27] and about 8 and 10 from zero-angle electron-impact data.[20,26] This ratio is given by the quantity $\rho^2(q^2+1)$, where ρ and q are defined in Ref. 27. A further analysis along the lines suggested by Fano and Cooper[27] cannot be reliably made to the present data because of the difficulty in drawing a background line through the resonance. This prevents us from estimating the parameter q for which the optical value[27] is -2.80 ± 0.27, and the zero-angle electron-impact result of Boersch *et al.*[28] is -2.83. The 1° result would appear to suggest a value on the order of -1, while it is virtually impossible to estimate a result for 2.7° unless the theoretical background shape is known. Further work is planned at higher resolution to study the angular dependence of this transition in more detail.

Other quantities of interest to this experiment are the cross-section differential with respect to energy loss, $d\sigma/dE$, and the total elastic, σ_{el}, and inelastic, σ_{inel}, cross sections. Unfortunately the angular grid was not fine enough and did not extend far enough into the small-angle region to make it possible to obtain reliable estimates of either $d\sigma/dE$ or σ_{inel}. Relative measurements of the elastic differential cross section by Geiger[29] were used to supplement our data in the small-angle limit. These data were placed on an absolute scale by matching to our results at 1.5° (see Fig. 6) and made it possible to obtain an estimate of the total elastic scattering cross section. Our experimental value of 0.00658 ± 0.00008 a.u. compares well with the theoretical value 0.00649 a.u. obtained from partial-wave calculations using the computer code of Yates[30] with a Hartree–Fock description of the atomic field.

All of the work reported here is in excellent agreement with the predictions of the first-Born theory of scattering. The measurements cover a region of sizable momentum transfer ($K^2 > 0.56$) and complement photoabsorption data ($K \to 0$) and the data for small K previously published by others.[20,26,29] The sheer number of experimental quantities found here to be in agreement with first-Born theory presents a strong argument to the effect that all the applications of the Bethe theory described in Inokuti's review article[1] can probably be experimentally realized, at least for the lighter elements. Extension of this work to other atomic and molecular systems is in progress.

---

*Work supported by Air Force Office of Scientific Research under Grant No. AFOSR-70-1900.

†Publication No. 2171 from the Chemical Laboratories of Indiana University, Bloomington, Ind. 47401.

[1]M. Inokuti, Rev. Mod. Phys. **43**, 297 (1971).

[2]R. A. Bonham and C. Tavard, J. Chem. Phys. (to be published).

[3]M. Inokuti and R. L. Platzman, in *Fourth International Conference on the Physics of Electronic and Atomic Collisions: Abstracts of Papers* (Science Bookcrafters, Hastings-on-Hudson, New York, 1965), p. 408; Argonne National Laboratory Report No. ANL-7060 1965, p. 7 (unpublished).

[4]H. Schmoranzer, R. C. Ulsh, R. A. Bonham, and J. Ely, J. Chem. Phys. (to be published).

[5]H. F. Wellenstein and R. A. Bonham, Phys. Rev. A 7, 1568 (1973).

[6]R. A. Bonham, Rec. Chem. Prog. **30,** 185 (1969).

[7]J. Geiger, Z. Phys. **177,** 138 (1964); Z. Phys. **175,** 530 (1963).

[8]H. F. Wellenstein and R. A. Bonham, Chem. Phys. Lett. **15,** 530 (1972).

[9]M. Cooper, Adv. Phys. **20,** 453 (1971). In addition to the results given on p. 461 also note that $\langle p^n \rangle = 2(n+1)\int_0^\infty dq \times q^n J(q)$, for $n \geq 0$, and that $J(q) = (1/2)[\langle 1/p \rangle - (1/2)q^2 \times 4\pi\rho(0) + O(q^4)]$, near the profile maximum.

[10]H. F. Wellenstein and H. Schmoranzer (unpublished).

[11]H. H. Steigerwald, Optik (Stuttg.) **5,** 469 (1949).

[12]H. F. Wellenstein and H. Schmoranzer (unpublished).

[13]A small source of systematic error was discovered in the angle measurement. The effect of this error, on the results presented here, is within the quoted experimental uncertainties. See Ref. 10 for details.

[14]C. Möllenstedt, Optik (Stuttg.) **5,** 499 (1949). For a description of an analyzer similar to the one employed here see, A. J. F. Metherell and M. J. Whelan, J. Appl. Phys. **37,** 1737 (1966).

[15]H. F. Wellenstein, J. Appl. Phys. (to be published).

[16]M. Fink and R. A. Bonham, Rev. Sci. Instrum. **41,** 389 (1970).

[17]R. A. Bonham and H. F. Wellenstein, J. Appl. Phys. (to be published).

[18]R. Kollath, Ann. Phys. (Paris) **27,** 721 (1936).

[19]W. J. B. Oldham, Phys. Rev. **186,** 52 (1969).

[20]S. M. Silverman and E. N. Lassettre, J. Chem. Phys. **40,** 1265 (1964).

[21]L. Vriens, in *Case Studies in Atomic Collision Physics I,* edited by E. W. McDaniel and M. R. C. McDowell (North-Holland, Amsterdam, 1970), Chap. 6, Sec. 6.5, p. 363.

[22]W. Huo (private communication).

[23]R. A. Bonham, Chem. Phys. Lett. (to be published). The generalized oscillator strength $f_n(K)$ can be regarded (Ref. 1) as a function of K^2 and hence can be expanded in a Taylor series about the value of K^2 at an average energy loss $\bar{E}$ as (a): $f_n(E_n, K) = f_n(E_n, \bar{K}) + (\bar{K}^2 - K^2)(\partial f_n[E_n, K]/\partial K^2)|_{K=\bar{K}} + \cdots$. Since an expansion of K^2 about the point $\bar{E}$ yields (b): $K^2 = k^2 + k^2(\bar{E}) + (\bar{E} - E) - 2k[k^2(\bar{E}) + (\bar{E} - E)]^{1/2} \cos\theta = \bar{K}^2 + (\bar{E} - E_n)^2 / 4k_n^2(\bar{E}) + O(1/k_n^4)$. Equation (12) follows immediately by summing both sides of (a), multiplied by E_n^μ, after interchanging the order of differentiation and summation in the correction term. Note also that $\bar{E}$ and $k(E)$ are replaced by their binary-encounter values, $k^2 \sin^2\theta$ and $k\cos\theta$, where necessary.

[24]Y.-K. Kim and M. Inokuti, Phys. Rev. **165,** 39 (1968).

[25]N. Oda, F. Nishimura, and S. Tahira, Phys. Rev. Lett. **24,** 42 (1970).

[26]H. Boersch, J. Geiger, and B. Schröder, Abh. Dtsch. Akad. Wiss. Berl. Kl. Math. Phys. Tech. 1, 75 (1967).

[27]U. Fano and J. W. Cooper, Phys. Rev. **137,** 1364 (1965).

[28]Our own estimate obtained from published intensity curves in Ref. 26.

[29]J. Geiger, Z. Phys. **175,** 530 (1963).

[30]A. C. Yates, Comput. Phys. Commun. **2,** 175 (1971).